Launching Graphene into 3D-Space: Symmetry, Topology, and Strategies for Bottom-Up Synthesis of Schwarzites

Alexey V. Ignatchenko*

Chemistry Department

St. John Fisher University

3690 East Avenue, Rochester, NY 14618, USA.

KEYWORDS: carbon nanomaterials • polycyclic aromatic hydrocarbons • organic synthesis • Schwarzites • chemical topology

ABSTRACT: Schwarzites are hypothetical carbon allotropes in the form of a continuous negatively curved surface with a three-dimensional periodicity. These materials of the future attract interest because of the expectation for their large surface area per volume, high porosity, tunable electric conductivity, and excellent mechanical strength combined with light weight. Three-decades long history attempting synthesize Schwarzites from the gas phase carbon atoms went without success. Design of Schwarzites is both digital art and science of placing tiles of sp^2-carbon polygons on mathematically defined triply periodic minimal surfaces. The knowledge of how to connect polygons in sequence using the rules of symmetry unlocks paths for the bottom-up synthesis of Schwarzites by organic chemistry methods. Schwarzite tiling by heptagons is systematically analyzed and classified by symmetry and topology. For the first time, complete plans for a bottom-up synthesis of many Schwarzites are demonstrated. A trimer of heptagons is suggested as the key building block for most synthetic schemes.

Introduction

The phenomenal rise of carbon allotropes such as graphene,[1] nanotubes,[2,3] and fullerenes,[4] has been continuously offering technological advances in various fields, including photovoltaics,[5,6] batteries and supercapacitors,[7–10] membranes,[11,12] gas separation and storage,[13] chemical catalysis,[14–16] and electronic sensors.[17–19] It is quite fortunate that carbon nanotubes, and fullerenes can be easily produced on industrial scale by "brute force" methods – precipitation of carbon from the gas phase using metal catalysts or via an electric discharge between carbon electrodes, and that graphene can be economically produced by exfoliation from natural graphite sources.[1–4]

Schwarzites, a particularly elusive form of carbon allotropes, have generated considerable excitement, although synthesis remains unrealized. Introduced by McKay and Terrones over three decades ago,[20] Schwarzites named after German mathematician Karl Hermann Amandus Schwarz are unique in their triple periodicity possessing a beautiful symmetry that continues to fascinate physicists and material scientists around the world. Like its cousins, these hypothetical carbon materials are supposed to consist of only sp^2-hybridized carbon atoms, with the striking difference that it would be a single piece of a continuous periodic surface filling in the whole 3D space. Access to Schwarzites would be analogous to achieving a tight packing of a single layer graphene in 3D space by bending, twisting, and fitting it in without cutting into pieces while enhancing its remarkable properties. According to numerous DFT calculations, Schwarzites might have superior mechanical strength, light weight, high porosity, gas permeability, combined with a tunable energy gap between the valence and conduction bands which graphene is lacking.

The synthesis of Schwarzites remains a challenging task that is fundamentally related to their negative Gaussian curvature. The spontaneous growth and termination of a positively curved surface of carbon atoms by closing to itself produces spherical fullerenes or cylindrical nanotubes as a converging process in which pieces with different curvature can be separated afterwards by fractionation. Growth at a constant zero curvature to a flat graphene is non-converging, therefore, infinite. In contrast, growth of a negatively curved triply periodic minimal surface (TPMS) from a gas phase carbon is infinite but diverging.[21] Even if it could be seeded with a negatively curved element, its subsequent growth is possible not just in one but many ways the exact number of which we do not know yet. Unlike fullerene spheres, TPMS growth does not terminate after surface edges meet creating a closure. Instead, it continues facing a vast number of options. It is not only a different curvature that may form, but also type of TPMS, or several types that might start growing simultaneously on different sides of a joined piece without a possibility for separation later. Not surprisingly, all attempts to grow spontaneously and hopes to isolate any Schwarzite in symmetrically pure state by brute force methods have failed. The difficulty extends to the zeolite templating method, in which even a smallest mismatch between crystal lattice parameters of the zeolite template and the Schwarzite, or presence of any residual hydrogen atoms inevitably leads to defects.[22,23]

Recent advances in the bottom-up synthesis of large size Polycyclic Aromatic Hydrocarbons (PAH) have created a foundation of synthetic methods which may apply to the construction of novel carbon-based compounds and materials with exciting new topologies beyond plane nanographenes.[24–26] However, bottom-up synthetic strategies for complete Schwarzite molecular architecture have not been discussed in literature. Currently, the only strategy for creating PAH with a negative curvature is narrowed down to occasional inclusion of heptagons or octagons between benzene rings.[26–31] The opposite approach suggested in this work is to use heptagons or octagons as building blocks and join them to construct benzene rings in-between. This study is intended to bring attention of synthetic organic chemists to the needs of the research

field traditionally dominated by solid state physicists and material scientists. The goal is to analyze the symmetry and topology of various Schwarzites that will allow to choose the best strategy and to guide their bottom-up synthesis by organic chemistry methods.

Results and Discussion

1. Topology.

Planning for a bottom-up synthesis of Schwarzites must start with a choice of a certain type of TPMS, the size of polygons, and a distinct tiling scheme. The most attractive synthetic targets are surfaces with a low genus and wider pores such as P, D, G, H, HT, CLP, GW, or IWP. Examples of an ideal surface are shown on Fig. 1 and tiling on various surfaces is illustrated throughout the paper. For the classification, description, and 3D models of TPMS, refer to websites of Ken Brakke [32] and Alan Shoen [33].

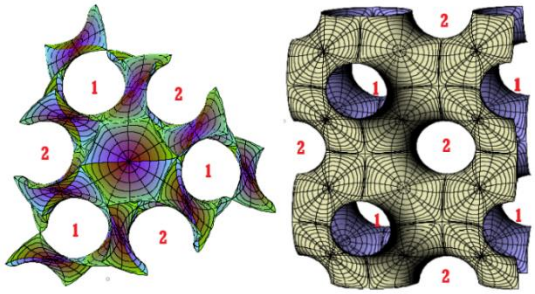

Figure 1. Balanced surfaces (G- and P- shown as examples) are recognized by two identical sides, 1 and 2, causing an equal size diameter of channels connecting neighboring chambers.

Polygon tiles contributing to a negative curvature, must have their size N larger than six atoms, i.e., N = 7, 8, 9, or higher, are suitable. [34] It is dictated by the Euler's equation (1)

$$V - E + F = 2(1 - g) \qquad (1)$$

wherein F, E, V are the number of faces (i.e., polygons), edges, and vertices, respectively. [34,35] Genus, g, is related to the number of handles, i.e., pairs of openings in the unit cell. In the special case when all atoms are sp^2 hybridized carbon, each atom has three sigma bonds. Three cycles share one atom, and two cycles share one edge (bond), so that 2E = 3V. In this case, Euler's rule prescribes a certain number of polygons in the unit cell of a closed periodic structure having genus g according to the equation (2). [35]

$$\sum_N (6 - N) f_N = 12(1 - g) \qquad (2)$$

For example, formula (2) predicts that $f_7 = 24$ heptagons (N=7) or $f_8 = 12$ octagons (N=8) will be required to construct a unit cell of the P-surface which has genus g=3. It may also be a combination of any size polygons, such as 4 octagons and 16 heptagons, or 26 heptagons and 2 pentagons. Pentagons create a positive curvature. Their presence is leveling off the negative curvature brought by polygons with N>6. Exactly twelve pentagons make spherical fullerenes according to equation (2) because sphere has genus zero. Hexagons are excluded from the calculation since the 6-N term in such case becomes zero, therefore, any number of hexagons may be used without affecting curvature. Consequently, dilution by any number of hexagons is allowed for the bottom-up synthesis of negatively curved Schwarzites while mixing heptagons or octagons with four or five-membered rings observed in some studies[31,36–40] is counterproductive.

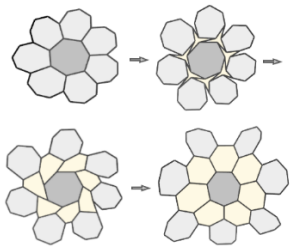

Figure 2. Leapfrog transformation[34] from condensed heptagons to the hyperbolic soccer ball pattern.

Non-diluted structures composed of only octagons or heptagons have been described in literature, [41–43] but their geometry looks highly strained for a carbon structure, and less accessible synthetically, similar to how C60 and C20 fullerenes are different. [44] The simplest way of isolating heptagons by dilution with minimum number of hexagons, is called "hyperbolic soccer ball" pattern (Fig. 2) which is like how pentagon rings in C60 fullerene are separated by hexagons. [45] A leapfrog transformation described by King [34] shows the relationship between heptagons-only pattern and the hyperbolic soccer ball. In organic synthesis, a hypothetical [2+2+2] cycloaddition of three molecules of cycloheptene would create a hexagon ring. It is to the great advantage of such bottom-up synthesis approach that no special care would be needed for creating hexagons – they will be created automatically by connecting six adjacent vertices of three heptagons. Thus, the hyperbolic soccer ball pattern, known by Schläfli symbol t{3,7}, or vertex symbol [6.6.7], [46] may become the preferred way to construct Schwarzites. It has been long recognized that a hyperbolic surface with genus three and 24 heptagons, i.e., 168 atoms, is equally important and analogous to the spheric surface fullerene that has 60 atoms. [34] Any further dilution by hexagons creates fullerenes with a higher number of atoms, such as C70, as well as Schwarzites with higher than 168 atoms in the unit cell for genus 3.

2. Symmetry.

Mathematically ideal TPMS from the P, G, D, family are said to be balanced when two sides of the surface are equal (Fig. 1). Two labyrinths on both sides of the balance surface created by the division of the whole space are congruent. Tiling may not always be perfectly symmetrical causing the distortion of the balance surface of tiles, hence, the symmetry reduction. Such distortion can be visually recognized by altering otherwise equal areas of openings 1 and 2 (Fig. 1) that would become larger and smaller. A balanced tiling tends to be of a higher symmetry. Examples include **P7par** [47], **P8** [20], **G8Bal**, and **D8Bal**. [48] Tiling can be chiral, as in **D168** [49], **P207-C168**, or **P130-C672** [45], regardless of being balanced or not (Table S1). The nomenclature for Schwarzites used in this work, in bold, consists of the TPMS type, the symmetry group, the chemical element symbol, and the number of atoms in the unit cell. For enantiomeric surfaces, (P) or (M) symbol may be added at the end depending on the positive (Plus) or negative (Minus) torsion angle of the propeller made of three heptagons located in corners of the cubic symmetry unit cell.

For TPMS with the cubic symmetry, such as P-, G-, or D-surface, balanced tiling is easier to accomplish with eight-membered polygons amenable to the C4 rotation symmetry of a cube. Tiling with seven-membered polygons more often makes unbalanced surface. Not surprisingly, the first discovered Schwarzite, MacKay-Terrones P-surface, was composed of octagons and it was balanced. [20] Related D- and G- surfaces based on octagon tiling were reported shortly thereafter. [48] Tiling of D-surface by heptagons in the

hyperbolic soccer ball pattern was described by Vanderbilt and Tersoff[49] in 1992, but it took another thirty years to find solution with the same pattern for P-surface. [45] G-Surface tiling by heptagons for the first time, is shown below. An up-to-date information on new Schwarzites can be found in the SACADA database. [50]

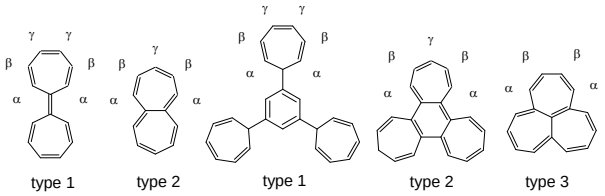

Figure 3. Types of heptagon dimers and trimers as building blocks for the bottom-up synthesis of Schwarzites, classified by their connection to each other through one, two or three vertices leaving alpha, beta, and gamma positions for interconnections.

To avoid the obvious mismatch between a single heptagon and the cubic unit cell symmetry, and to facilitate synthesis by using preassembled larger size building blocks, heptagons can be combined in dimers and trimers (Fig. 3). Trimers must be placed on each of eight corners of the cube and can be oriented according to the four C3 rotation axes, as for example on **P207-C168** (Fig. 4). At the same time, unit cell tiling by heptagons can be viewed as placing pair of dimers on each of the six faces of the cube and orienting them to obey C4 rotation symmetry. Either way, 8x3 or 6x4 tiling, brings the same result, 24 heptagons, according to the total number required by the Euler's formula (2) for the unit cell.

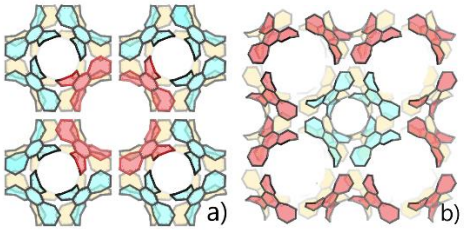

Figure 4. a) Half of the **P207-C168**[45] (unbalanced) surface large chamber is seen in the center between four small chambers (in axial plane, or eight in 3D). In return, b) small chamber is surrounded by eight large chambers. The surface serves as the border between chambers so that all small chambers are on one side while large chambers are on the other side of the unbalanced surface.

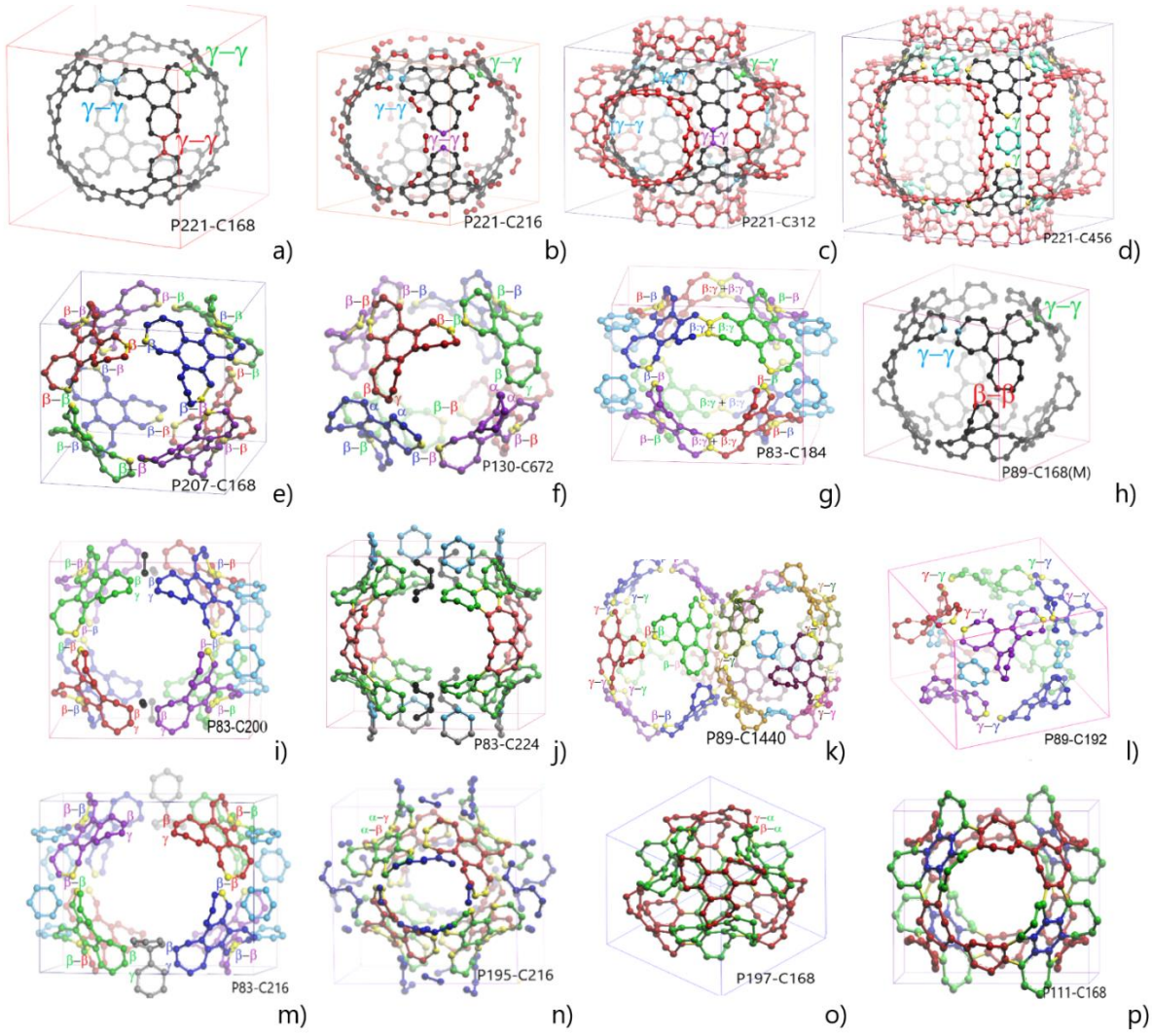

Figure 5. P-Schwarzite tilings variety made by rotating type 2 heptagon trimers in eight corners of the unit cell while changing trimers connection to each other through alpha, beta, or gamma carbon atoms.

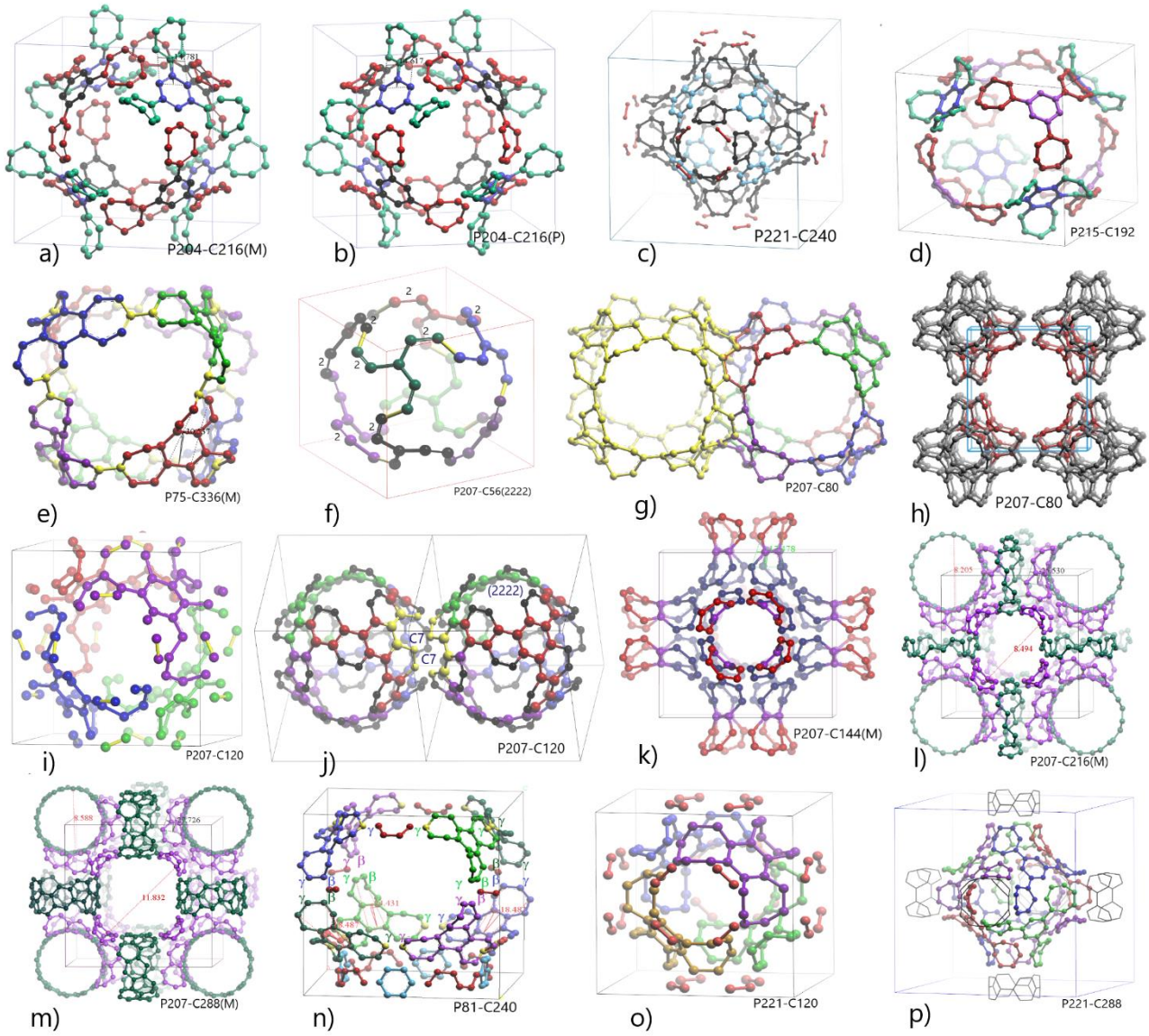

Figure 6. Various P-Schwarzite tilings made by a-d), p) type 1, e), n) type 2, and g) type 3 heptagon trimers, or k-m) by heptagon dimers, or through sharing edges of f-j) heptagons or o) octagons. Achiral Schwarzites, like **P204-C216**, may have chiral tilings, like enantiomeric (M) and (P) pair, a-b).

The narrowest place of P-surface is where two chambers join the edges of their openings creating a neck (Fig. 1). Let's introduce a topological characteristic of edges composing the neck useful for the net with point symbol {6.6.7}. If we define it as the number of carbon atoms on each heptagon of the chamber's opening exposed for the connection with another chamber (Fig. 4a), all six openings of **P207-C168** small chamber will have the same configuration, (2222). Continuity of the net with the same point symbol, i.e., by making hexagons between heptagons dictates the configuration of the joined neighboring chamber also to be (2222) which classifies this configuration as self-complementary. While **P207-C168** is chiral, the neck configuration is not as it will be explained below.

Other examples of self-complementary configurations for joining two cyclic chains of four heptagons are achiral (3131), chiral (3122), or chiral (4112), while (3311) taken as an example, is not self-complementary because it requires (4121) to be paired with it when making hexagons in between two chains. These statements can be easily verified on paper by drawing the above configurations. Neck configuration is cyclically permuted, i.e., it may be written starting from any position forward in a circular way, while writing in reverse order represents a mirror image. For example, writing (3122) is the same as (2312) while (3221) is their enantiomer. If the reverse writing makes a different sequence from the original, it indicates chirality. For consistency, counting should be done in the same way, for example, clockwise when viewing the chamber from outside, in reverse lexicographic order, listing larger numbers first.

Self-complementary neck configurations are of a particular importance for the design of Schwarzites as the condition for periodicity by translational symmetry. Self-complementary configurations for five heptagons include achiral (22222), chiral (31222), chiral (32122), chiral (31312), and achiral (33121). The achiral (33121) configuration is seen in the chiral **P130-C672** [45] model because neck chirality is sufficient but not necessary requirement for the whole chamber or unit cell chirality. A partial list for self-complementary configurations with six heptagons is shown in the supporting information.

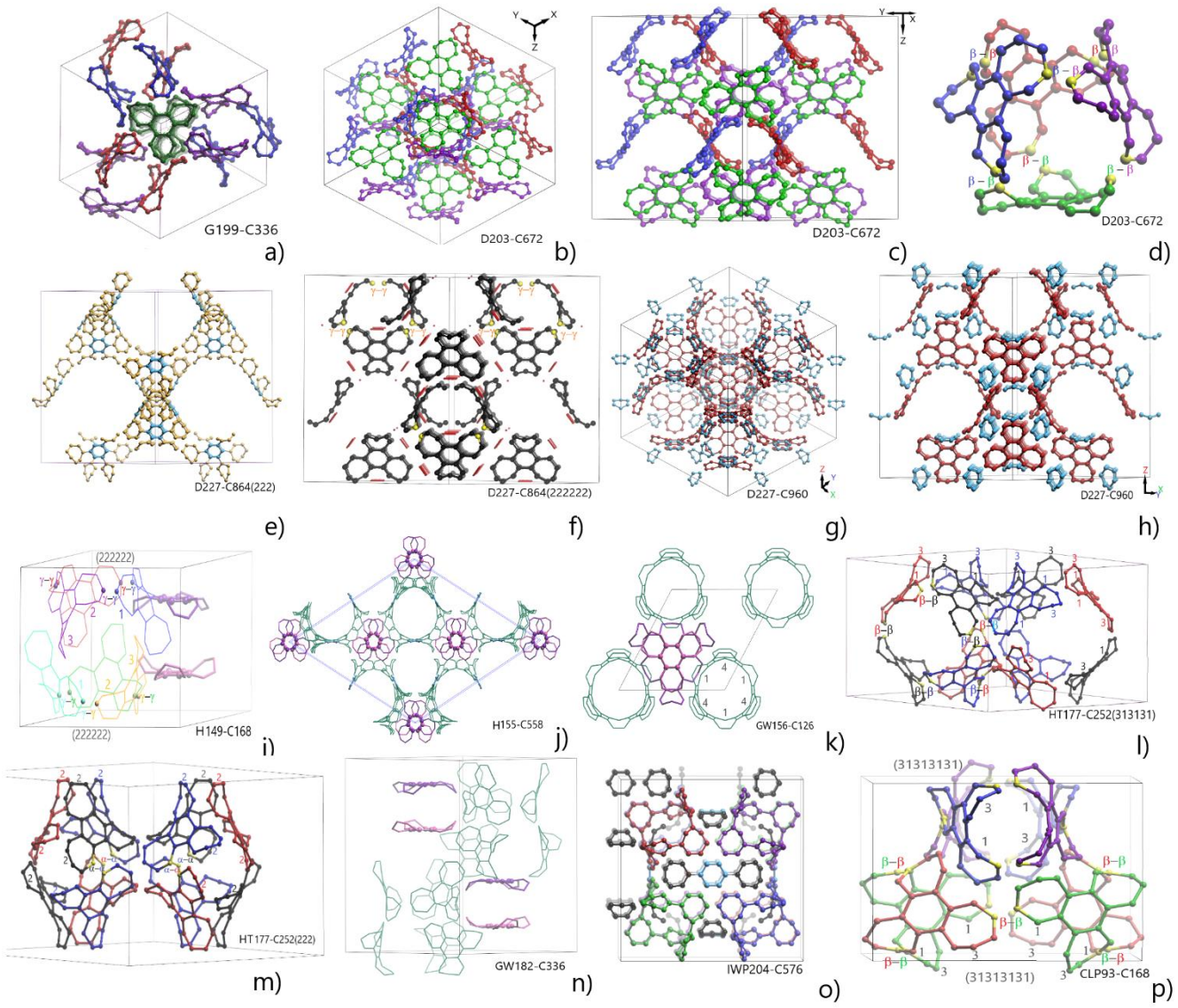

Figure 7. Examples of G, D, H, HT, GW, IWP, and CLP Schwarzites using heptagon trimers type 2, a) **G199-C336**, b-c) **D203-C672**, ref.[49] unit cell views, d) single chamber, e) type 1 **D227-C864(222)** f) type 2, **D227-C864(222222)** ref.[47] also called **D227-C216** ref.[45] g) type 2, **D227-C960**, h) **CLP131-C216**, i-n) various hexagonal Schwarzites with channels made of trimers (shown in green) linked by trimer pairs (shown in purple), o) **IWP204-C576**, p) **CLP93-C168**

A variety of P-surface tilings can be obtained by rotating heptagon trimers in eight corners of the unit cell cube and connecting them through either alpha, beta, or gamma positions (Table S1, Fig. 5-6). The most symmetrical is gamma-to-gamma connection within the unit cell for all three heptagons of the type 2 trimer (defined on Fig.3) leading to $Pm\bar{3}m$ symmetry, group 221. The remaining two carbon atoms, alpha and beta, from each four trimers on cube's face make (22222222) chamber neck configuration to be used for connecting with neighboring chambers, while beta-to-beta connection would create less symmetrical (31313131) configuration. The former case requires skewing to match positions of K-region of one chamber opening and bay-regions of another chamber. Without skewing, direct contacts between both chamber's opposite K-regions create **P221-C168** with C4 and C8 rings between unit cells (Fig. 5a), synthetically a very challenging structure which departs from the hyperbolic soccer ball pattern. The skewed structure creates a pair of enantiomers of **P207-C168-γ** while reducing symmetry to P432, group 207, and introducing chirality. Found to be highly strained and unstable by DFT calculations this structure undergoes skeletal rearrangements. Therefore, tiling by gamma-to-gamma connections should materialize by adding more hexagons, for example, joining bay-regions via shared C2 fragment (**P221-C216**), or extra C6 rings (**P221-C312**, **P221-C456**, (Fig. 5b-d), or any number of additional C6 rings creating many more new tilings.

When type 2 heptagon trimers rotate in each corner of the cube, the symmetry is reduced, naturally more stable tilings are produced via beta-to-beta connection either as the only type, creating (31313131) neck configuration of **P207-C168** (Fig. 5e), **P200-C276** (Fig. S1i-j), or mixing β–β and γ–γ connections as in **P130-C672**, **P89-C168**, **P89-C192**, **P89-C1440**, sharing β–γ edge, **P83-C184**, **P83-C224**, separating β–γ edges by dilution, **P83-C200**, **P83-C216**, (Fig. 5f-m), or using alpha positions for chiral **P195-C216**, and **P197-C168** (Fig. 5n,o). A curious case is when two different kinds of chiral chamber in a group of eight in the unit cell create four diastereomers of **P89-C1440** (Table S1). Another interesting case is

meso-chirality of **P111-C168** that has a symmetry plane through pairs of chiral heptagons in each trimer which renders this Schwarzite achiral. Noteworthy, it utilizes another trimer type, 1,3-disubstituted C7-ring, by mixing it with type 2 shown in red and blue-green colors, respectively (Fig. 5p). Similarly, rotation of type 1 trimers of the balanced chiral tiling **P204-C216** makes unbalanced achiral **P221-C240**, or **P221-C288** (Fig. 6a-c,p) with (2222) neck configuration for inter-chamber connections. Type 1 and type 2 trimers can be mixed as in **P215-C192** (Fig. 6d). Heptagon dimers sharing edges are utilized in chiral Schwarzites **P207-C120**, **P207-C144**, **P207-C216**, **P207-C288** (Fig. 6i-m). Some Schwarzites with edge shared heptagons, **P207-C80**, or octagons, **P207-C56**, **P221-C120**, (Fig. 6f-h,o) may not allow tiling by trimers or dimers. In summary, variation of tilings can be obtained by adding hexagons, varying dimers and trimers type, and their orientation in the cubic unit cell.

Each P-surface tiling has associated D- and G-surface tilings related through Bonnet rotation. For example, video 1 shows Bonnet transformation of **P197-C168** to **G199-C336** (Fig. 7a). A systematic study of Schwarzites relationship through Bonnet rotation will be reported separately. Selected examples of D, G, GW, H, HT, IWP, and CLP Schwarzites are shown on Fig. 7.

Like P-surface, switching between beta-to-beta and gamma-to-gamma connection of type 2 trimers and their dilution by hexagons can be applied to other surfaces. For example, dilution by hexagons in **D227-C864(222222)** or **CLP131-C216** (Fig. 7f,h) helps to avoid skewing and strain. Beta-to-beta connection creates **D203-C672** or **CLP93-C168** (Fig. 7b-d,p) without dilution. Dilution is component of type 1 trimer, **D227-C864(222)** (Fig. 7e), **P221-C240**, **P204-C216** (Fig. 6a-c) and **IWP204-C576** (Fig. 7o). It can be applied to any tiling, even beta-to-beta connected trimers, **D227-C960** (Fig. 7g).

Remarkably, symmetry allows the number of beta-to-beta connected trimers in opposite openings of a chamber to be 2, 3, 4, or 6 switching symmetries from cubic to hexagonal and the surface type between **CLP93-C168**, **GW177-C252(313131)**, **P207-C168**, **GW177-C252(222)**, respectively, with the same neck configuration (31313131) for the rest of openings (Fig. 8). Similar array of tilings exists for gamma-to-gamma connection of trimers which requires their dilution.

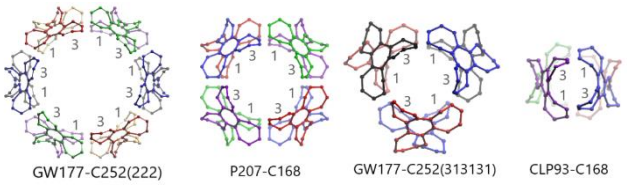

Figure 8. Number of beta-to-beta-connected trimers in a pair of chamber's opposite openings controls the surface type and symmetry.

3. Synthetic strategies.

3.1. P-Surface

Synthesizing PAH with rings larger than six atoms is a challenge affecting Schwarzites as well. Octagon-tiled Schwarzites are highly symmetrical and balanced, while heptagon is not an easy-to-fit tile for the cubic symmetry possessed by most TPMS. Application of dimers and condensed trimers (type 3, Fig. 3) not only satisfies symmetry, but also solves the problem of unpaired p-orbitals in the all-sp^2 heptagon hydrocarbon. For two other types of trimers, one or three carbon atoms with unpaired p-orbitals must be temporarily replaced by sp^3 atoms during the synthesis.

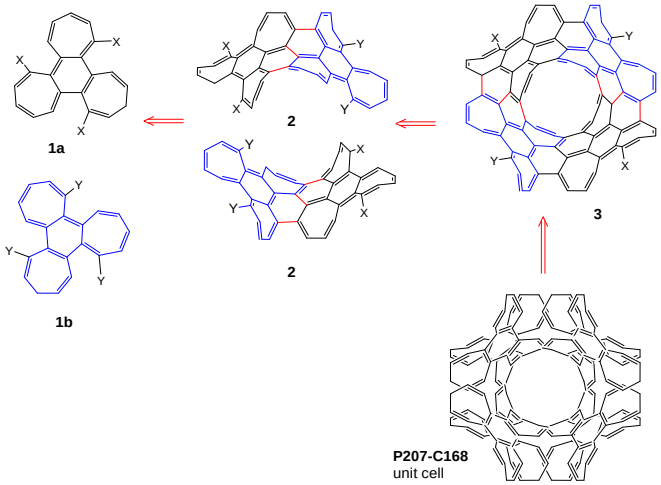

Scheme 1. P207-C168 Small chamber construction strategy by Method 1.

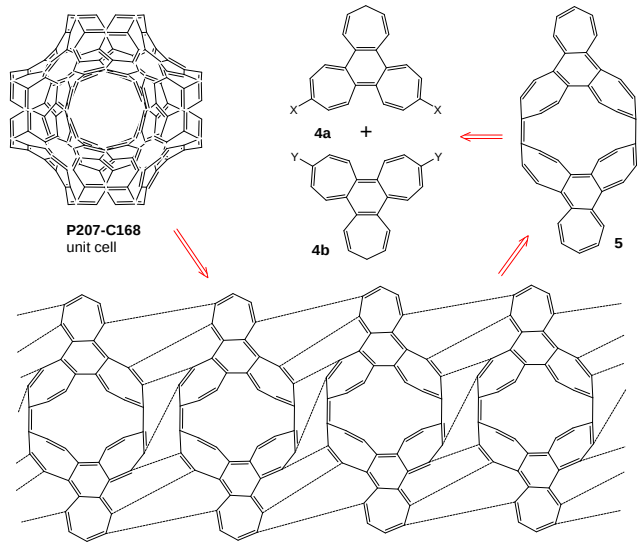

Scheme 2. Alternative strategy for P207-C168 small chamber synthesis by method 2, cross-coupling heptagon trimers and subsequent pairing through a radical domino process.

While chambers of a balanced surface are uniformly sized, construction of unbalanced surfaces may start with either a large or small chamber. The other size is created automatically as exemplified through **P207-C168** Schwarzite[45] (Fig. 4). Symmetry evokes several options for its assembly (Schemes 1-2). The size of the building block is doubled from one to eight trimers in three steps of Method 1 using cross-coupling reaction between X and Y linking groups. Method 2 links trimers via para-to-para positions during the first cyclization followed by radical domino process[51] for sequential dimerization and the final cyclization during the unit cell assembly (Scheme 2).

The final most challenging task is to stack unit cell cubes in close packed layers by connecting chamber's openings, often three pairs at once, according to the Terrace-Step-Kink (TSK) model.[52] Periodic organic material growth through precise covalent bonding with monomers in solution is unprecedented and significantly different from polymerization, crystals growth, or solvothermal synthesis of metal organic frameworks. The latter proceed with a low concentration of defects because of the reversible binding, unlike permanent covalent binding. Significant amount of trial-and-error work lies ahead for testing different ideas. One example is elimination of neighboring Me_3Si- and CF_3SO_3- groups to generate triple bonds by

Kobayashi's method[53–55], and connect alkynyl carbons in a cascade zipping reaction (Scheme 3). While there was no such precedent in literature, this reaction has a reasonable expectation to proceed based on the constrain of each alkyne bond position in space essential for cascade cyclization reactions.[56] Because of the stepwise cascade mechanism, the Hückel's 4N+2 rule for concerted electrocyclic reactions does not apply in this case.

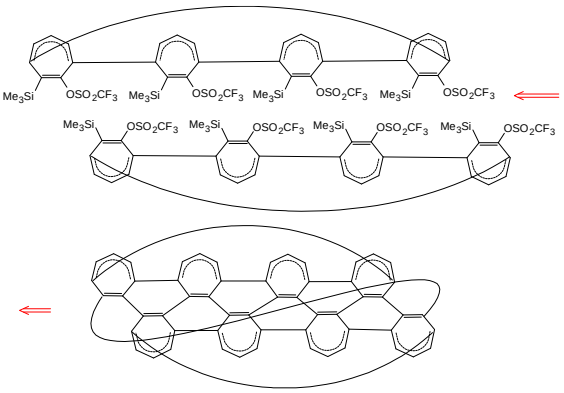

Scheme 3. Potential extension of Kobayashi's method of alkynes generation in situ for joining small chambers of P207-C168, neck configuration (2222).

P207-C168 Large chamber with achiral neck configuration (313131)^6 can be made by method 1 (Scheme 4) via beta-to-beta connection of trimers. The whole surface is chiral and chiral heptagon trimers must be used for its construction in a pure enantiomeric form. Fast racemization of propeller-like trimers with chirality defined by the torsion angle on Fig. 9 is expected in solution due to a shallow inversion barrier reminiscent of [7]-circulene.[57] Racemization becomes impossible when enantiomers configuration is fixed through step 2 cyclization. The chirality challenge adds up to the complexity of Schwarzites synthesis. Mixing up enantiomers violates the symmetry and makes growth in the desired direction impossible. The best strategy is to separate enantiomers after step 1 when larger fragments get higher inversion barrier, or after step 2 when racemization becomes impossible (Fig. 10).

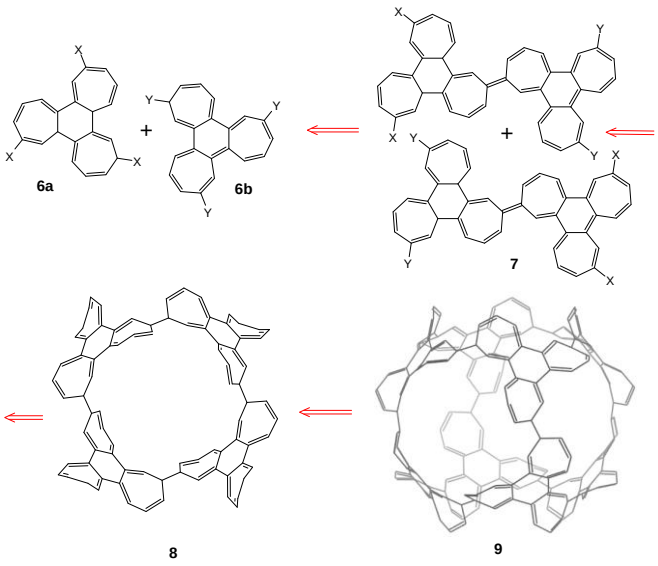

Scheme 4. Proposed synthesis of the P207-C168 large chamber by method 1.

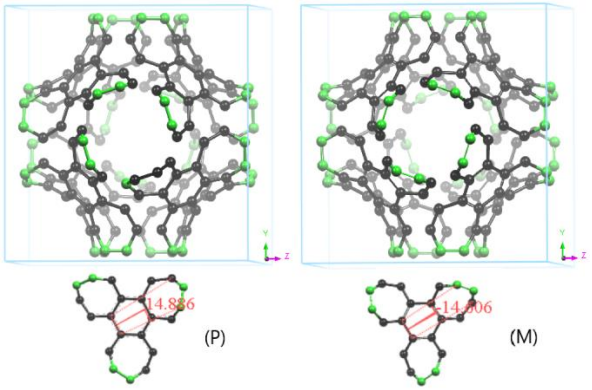

Figure 9. (P) and (M) enantiomers of hexagon trimers from **P207-C168** characterized by a positive (Plus) and negative (Minus) torsion defined as shown for the propeller-like shape, +14.8° and -14.8°, respectively.

A point system can quantify complexity of a synthetic design. Assigning one point for each cyclization step and one for managing chirality, the complexity index for both methods 1-2 in producing **P207-C168** is three. To minimize the number of cyclization steps, a simpler method could initially join four trimers, making two sets (**10a** and **10b** on Scheme 5) positioned at opposite corners of the unit cell cube body diagonal.

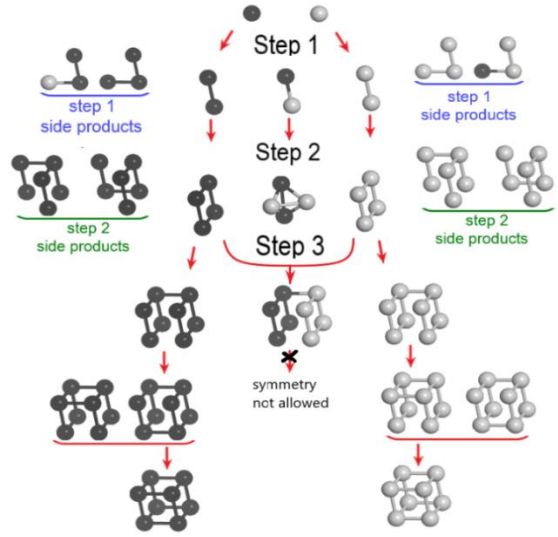

Figure 10. Stepwise construction of a chiral surface by method 1 requires separation of enantiomers. Dark and light balls stand for two enantiomers of the heptagon trimer building block.

Both intermediates **10ab** assume spherical shapes resembling half chambers during geometry optimization via molecular mechanics. By coupling two sets the entire chamber can be formed in a single cyclization bringing the complexity index down to two. Another advantage of method 3 is the ability to control selectivity of each group of four trimers formation by varying the ratio 1a:1b. A 3:1 excess of either trimer selectively creates **10a** or **10b** intermediate, while methods 1-2 may suffer from competing linear oligomerization alongside cyclization.

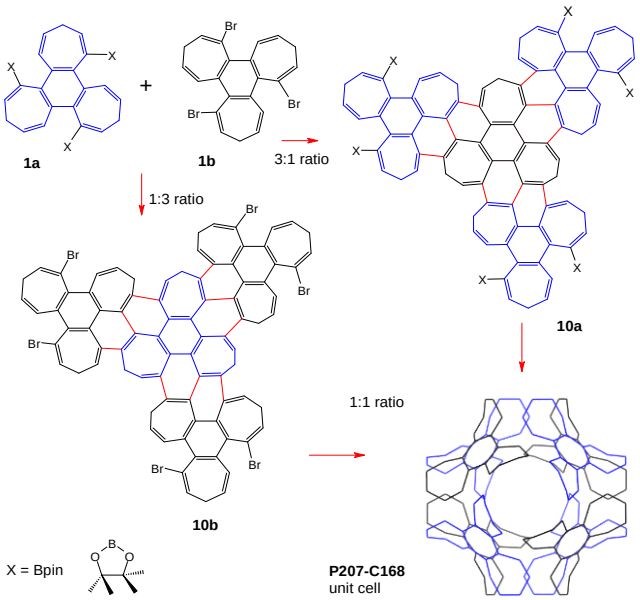

Scheme 5. Method 3 for the P207-C168 (chiral) small chamber construction.

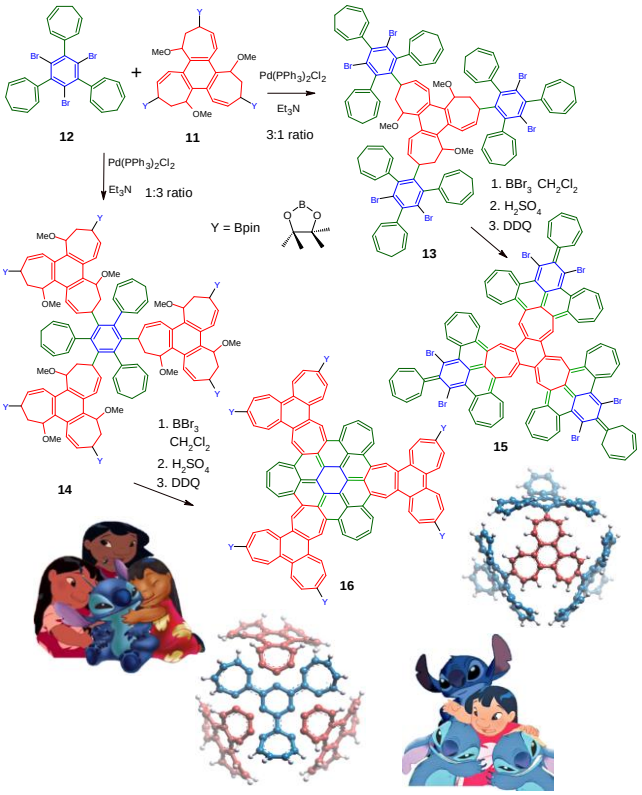

Scheme 6. Proposed construction of two halves of the P215-C192 unit cell from two kinds of trimers applying a principle of excess of one over the other. Nicknamed "Lilo and Stitch"[58], three trimers of each type surround the other one as illustrated here.

Application of method 3 for achiral Schwarzite synthesis, such as **P215-C192** (Scheme 6), brings the complexity down to 1. Six bonds must be created during the single cyclization step (Scheme 7). Molecular modeling shows that two intermediates, **15** and **16**, adopt the hemisphere shape required for cyclization after aromatization of not-so-much curved **13** and **14**. Both reactions can be done in one pot since there is a literature precedent of $Pd(OAc)_2$ catalyzed oxidative Heck process coupled with dehydrogenation by DDQ.[59] Each of the two types of trimers in **P215-C192**, structures **11** and **12** dubbed by students in our lab "Lilo and Stitch"[58] are surrounded by three trimers of the other kind as emphasized through illustration on Scheme 6. Worth mentioning, there are achiral Schwarzites, **P204-C216**, **P221-C240**, **P221-C288**, but their tiling is chiral with two options of different enantiomeric trimers of type 1.

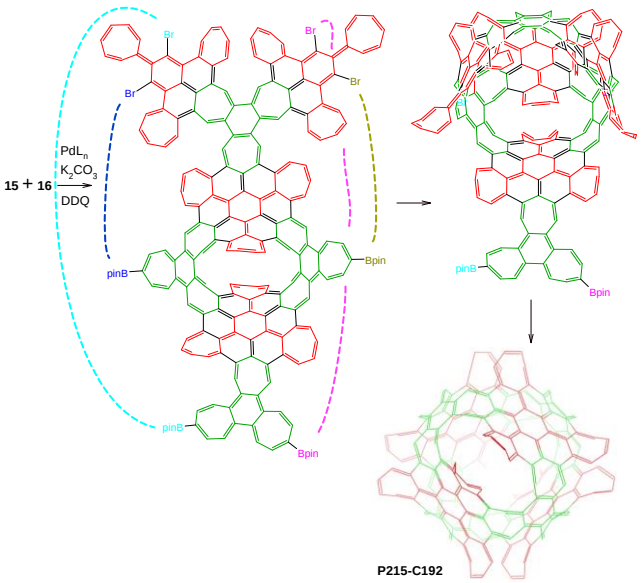

Scheme 7. Cyclization step for the P215-C192 Unit cell assembly.

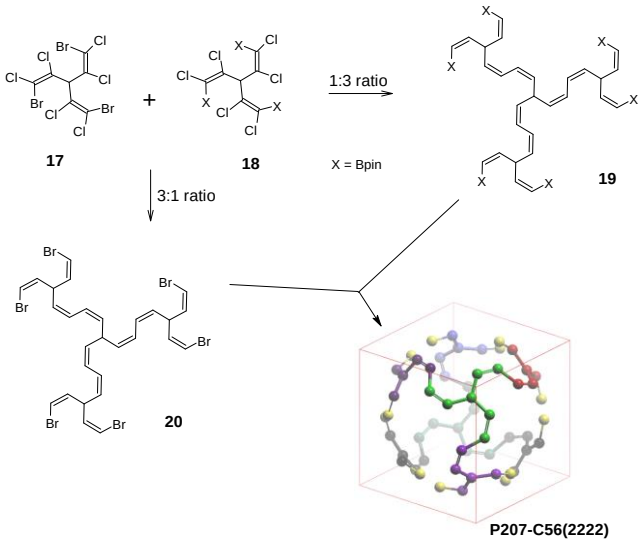

Scheme 8. Proposed synthetic design of the P207-C56(2222) large chamber by method 3. Chlorine atoms (omitted for clear viewing) are essential for joining unit cells into periodic structure.

Method 3 is applicable to other Schwarzites synthesis, even looking so challenging as **P207-C56(2222)** composed of octagons sharing edges (Fig. 6f, Scheme 8). The unit cell synthesis in this case gets complexity index 1, but it must create octagons when joining unit cells, possibly, by the Ullmann reaction, as well as dehydrogenate sp^3 atoms in each corner of the unit cell. Interestingly, changing the trans position of Br atom to the cis makes **P207-C56(1^8)** Schwarzite (Scheme S2), which is unstable according to DFT computation.

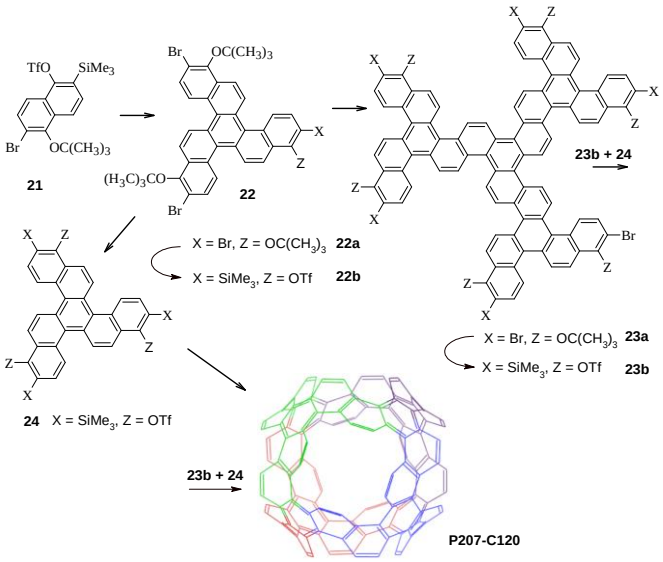

Scheme 9. Proposed synthesis of the P207-C120 large chamber through benzyne trimerization, stepwise via 23b, or directly from four molecules 24.

In a variation of method 3 applied for **P207-C120** synthesis design, cyclization may take place between two unequally sized pieces, **23b** and **24**, prepared through benzyne trimerization (Scheme 9). It might be possible to make **P207-C120** unit cell in one-pot reaction starting from trimer **24**, or even monomer **21**. Schemes 8-9 both imply C7 rings formation only during the step of joining unit cells.

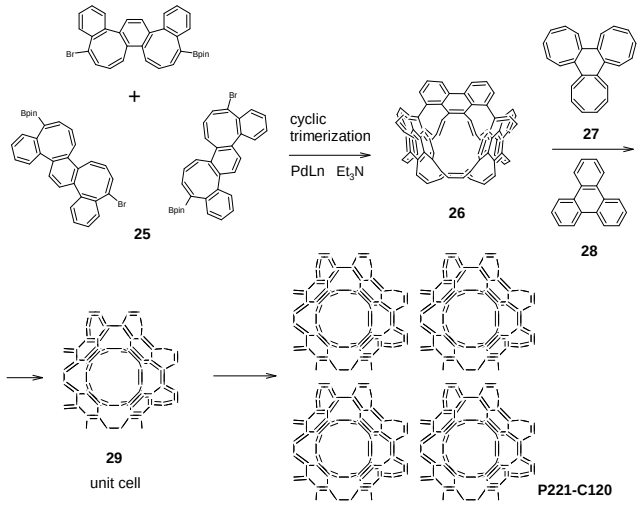

Scheme 10. P221-C120 Design.

Octagons too can be combined in trimers and spaced out at the four diagonal corners of the cube totaling twelve heptagons in the unit cell according to Euler's formula. C2 Fragments added between unit cells of **P221-C120** (shown in red, Fig. 6o) must stay on just three faces of the cube making unsymmetrical chambers difficult but still possible to synthesize (Scheme 10). A plan of complexity 3 suggests joining three dimers **25** into the first cycle of six octagons, then adding two nonequal size trimers as top and bottom covers. The last three octagons result from adding the small cover, **28**. Another way for dealing with unsymmetrical chambers is to make one larger than the unit cell (Scheme 11). Four dimers **30** create a barrel, **33**. Three barrels join through benzyne trimerization into half-chamber. Two half-chambers join into small chamber **35** serving as the periodic super-element and easing off TSK limitations. Tilings shown on Fig. 5-7 suggest synthetic designs for most other Schwarzites.

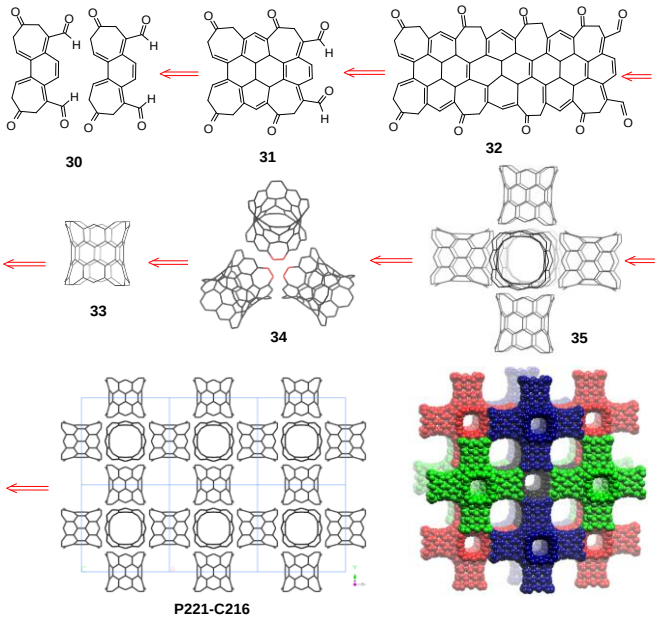

Scheme 11. P221-C216 Design.

3.2. D-Surface

Making the whole chamber, large or small, in just one cyclization is proposed for **D227-C960** construction (Scheme 12) using Suzuki-coupling and Diels-Alder benzyne condensation for gamma-to-gamma or alpha-to-alpha trimers **36**, **41**, connection, respectively, with the synthesis complexity at level 1. Dehydrogenation of the Diels-Alder product with DDQ is required for aromatization.

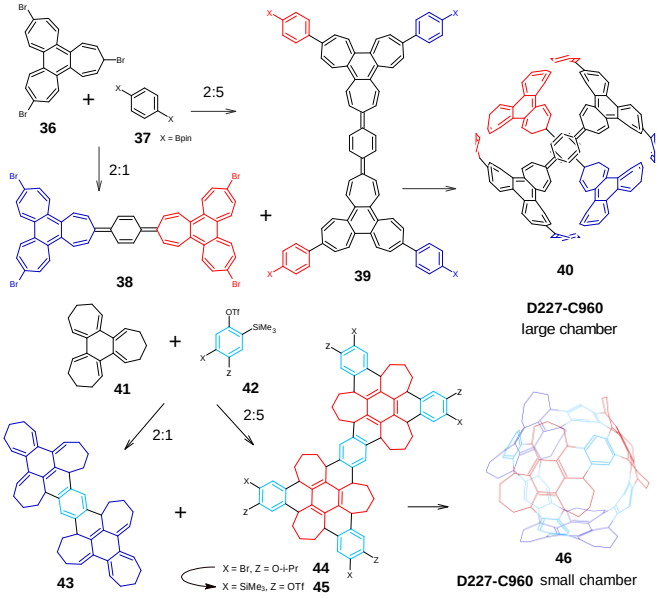

Scheme 12. D227-C960 chambers design.

P, D, and G-chambers constructed by gamma-to-gamma trimers connection can be joined by various length (n,n) armchair nanotubes offering infinite number of molecular architectures. Two strategies shown on Schemes 13-14 use [6]-cycloparaphenylene **50** for **D227-C1248**, or C2 fragments built in trimers **51-52** for **D227-C864(222222)** synthesis. Benzyne Diels-Alder reaction is proposed for attaching nanotubes to chambers. Additional examples of molecular architectures with nanotubes are shown in Supporting Information.

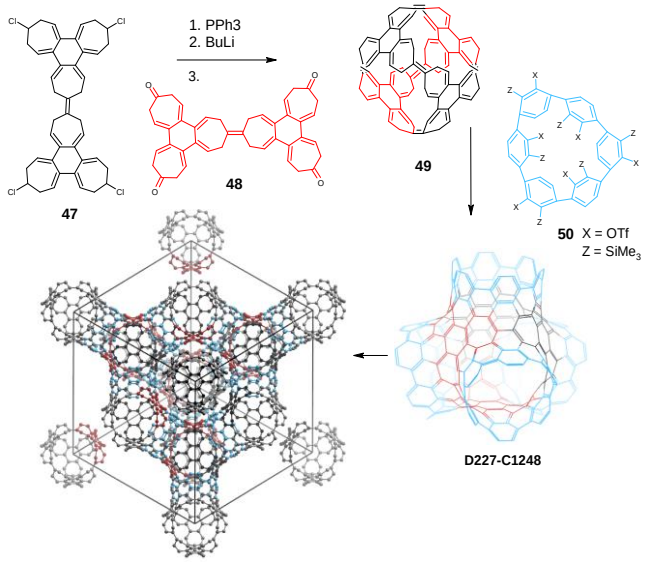

Scheme 13. D227-C1248 synthesis design via Diels-Alder condensation.

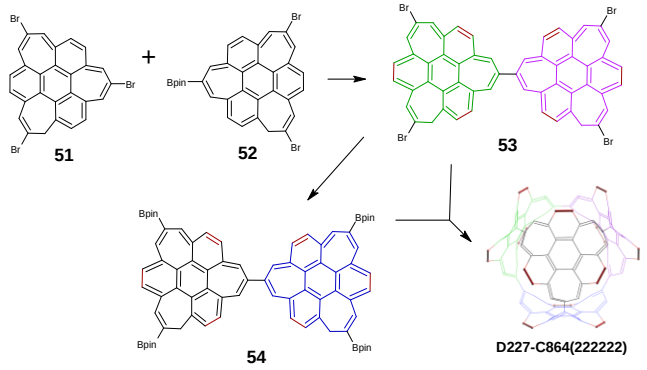

Scheme 14. Design for D227-C864(222222) synthesis via Suzuki-coupling.

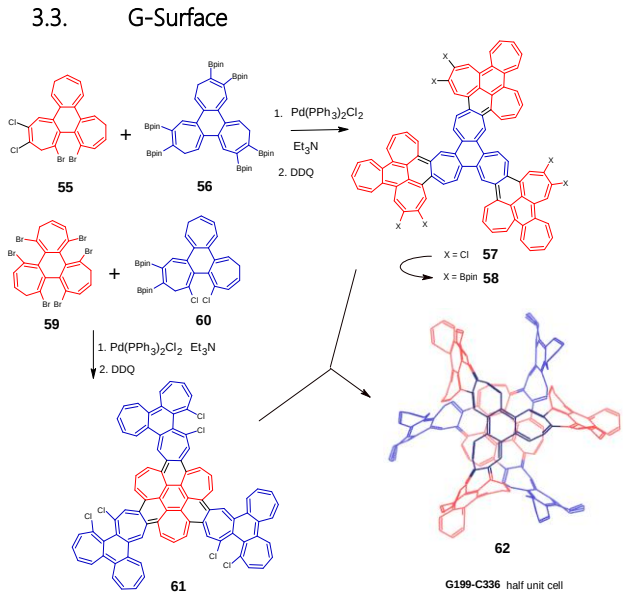

Scheme 15. G199-C336 chamber, half unit cell, design.

Classification of the connection type between trimers in P-chambers extends to G-surface. Thus, α:α + β:γ type seen in **P197-C168** can be used for making related (via Bonnet rotation) G-Shwarzite **G199-C336** by method 3 (Scheme 15), joining trimers **55** and **56** in 3:1 ratio into half-chamber **57** and pairing with the other similarly constructed half-chamber, **61**.

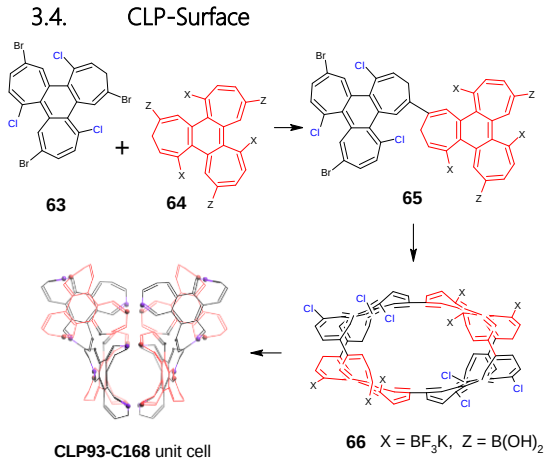

Scheme 16. CLP93-C168 chamber design.

Synthetic design of the simplest representative, **CLP93-C168** chamber (Scheme 16), proposes one cyclization between type 2 trimer beta carbons taking advantage of a higher reactivity of bromine vs. chlorine and $B(OH)_2$ vs. BF_3K in Suzuki-Miyaura coupling.[60] Less reactive groups will be utilized for joining chambers together while the rest of the bonds can be accomplished by dehydrogenation. Dilution by hexagons **(CLP131-C216**, Scheme S5) requires a larger set of building blocks and higher complexity.

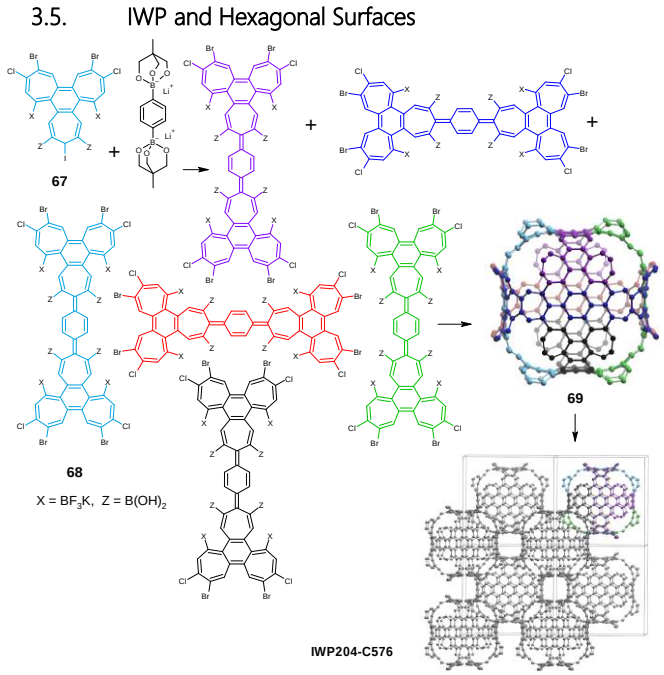

Scheme 17. IWP204-C576 Design.

Synthesis of **IWP204-C576** chamber might be possible from a single monomer **68** using different reactivity groups in stages. Less reactive Cl and BF_3K will be used for the final stage connecting cube corners into periodic structure (Scheme 17).

As a general strategy for Hexagonal Schwarzites each chamber connects to three others. **GW156-C126** Chamber can be prepared by joining two groups of six heptagons. Chambers **72** are linked by heptagon dimers **73** to form periodic structure (Scheme 18). A great

variety of hexagonal H, HT, GW Schwarzites, can be made by varying chambers and linking units (Table S1).

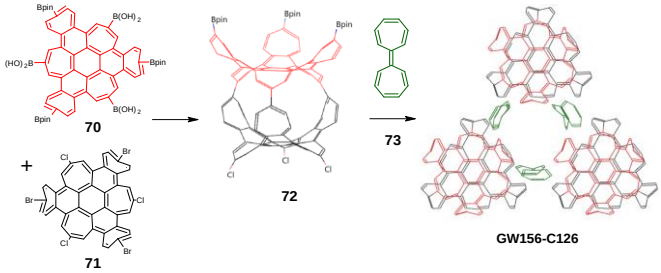

Scheme 18. GW156-C126 Design.

Summarizing synthetic methods, Diels-Alder and radical domino additions, Ullmann, Suzuki, and Heck couplings, can be used for making Schwarzites, apart from Scholl reaction,[26,27] which may cause C7-ring opening.

Conclusion

Systematically performed analysis of Schwarzites demonstrates that the bottom-up synthesis utilizing strategically selected heptagon or octagon trimers, holds greater potential for controlling wider array of topology, geometry, and pore size distribution in periodic carbon materials compared to templating on zeolites. Specific synthetic approaches must be devised and tested, with the major challenge being the assembly of chambers into periodic structures. Understanding topology and symmetry provides with guiding principles needed to succeed in synthesis.

ASSOCIATED CONTENT

Supporting Information contains DFT computational method, partial list of self-complementary neck configurations, table with the list of Schwarzites and data on their symmetry, geometry and topology, additional figures of some Schwarzites and synthetic schemes, identification of hexagonal Schwarzites, and molecular architectures extended with nanotubes. "This material is available free of charge via the Internet at http://pubs.acs.org."

AUTHOR INFORMATION

Corresponding Author

* aignatchenko@sjf.edu; Alexey.Ignatchenko@gmail.com .

Funding Sources

NSF grant 1955130

Notes

Any additional relevant notes should be placed here.

ACKNOWLEDGMENT

I dedicate my work in memory of scientists suffered from wars. I am grateful for the support and resources received from St. John Fisher University (SJF), the Lavery library, and the Chemistry department. I deeply thank Dr. Ken Brakke (Susquehanna University Prof. Emeritus), Dr. Mark McKinzie (Math Dept., SJF), Sam Acosta (2023 SJF graduate with B.S. degree in math), Dr. Humberto Terrones (Rensselaer Polytechnic Institute) for useful discussions and help with modeling. Support from the NSF grant 1955130 for the shared use of Materials Studio software and a high-performance computer is greatly acknowledged.

ABBREVIATIONS

TPMS, triply periodic minimal surface; PAH, Polycyclic Aromatic Hydrocarbons; DFT, density functional theory; TSK, Terrace-Step-Kink.

REFERENCES

(1) Urade, A. R.; Lahiri, I.; Suresh, K. S. Graphene Properties, Synthesis and Applications: A Review. *JOM* **2023**, *75* (3), 614–630. https://doi.org/10.1007/s11837-022-05505-8.

(2) Anzar, N.; Hasan, R.; Tyagi, M.; Yadav, N.; Narang, J. Carbon Nanotube - A Review on Synthesis, Properties and Plethora of Applications in the Field of Biomedical Science. *Sensors International* **2020**, *1*, 100003. https://doi.org/https://doi.org/10.1016/j.sintl.2020.100003.

(3) Rathinavel, S.; Priyadharshini, K.; Panda, D. A Review on Carbon Nanotube: An Overview of Synthesis, Properties, Functionalization, Characterization, and the Application. *Materials Science and Engineering: B* **2021**, *268*, 115095. https://doi.org/https://doi.org/10.1016/j.mseb.2021.115095.

(4) Yadav, J. Fullerene: Properties, Synthesis and Application. *Res. Rev. J. Phys* **2018**, *6* (3), 1–6.

(5) Ganesamoorthy, R.; Sathiyan, G.; Sakthivel, P. Review: Fullerene Based Acceptors for Efficient Bulk Heterojunction Organic Solar Cell Applications. *Solar Energy Materials and Solar Cells* **2017**, *161*, 102–148. https://doi.org/https://doi.org/10.1016/j.solmat.2016.11.024.

(6) Kumari, M. A.; Swetha, T.; Singh, S. P. Fullerene Derivatives: A Review on Perovskite Solar Cells. *Materials Express* **2018**, *8* (5), 389–406.

(7) Balogun, M.-S.; Luo, Y.; Qiu, W.; Liu, P.; Tong, Y. A Review of Carbon Materials and Their Composites with Alloy Metals for Sodium Ion Battery Anodes. *Carbon N Y* **2016**, *98*, 162–178. https://doi.org/https://doi.org/10.1016/j.carbon.2015.09.091.

(8) Cheng, Q.; Tang, J.; Ma, J.; Zhang, H.; Shinya, N.; Qin, L.-C. Graphene and Carbon Nanotube Composite Electrodes for Supercapacitors with Ultra-High Energy Density. *Phys. Chem. Chem. Phys.* **2011**, *13* (39), 17615–17624. https://doi.org/10.1039/C1CP21910C.

(9) Kumar, H.; Sharma, R.; Yadav, A.; Kumari, R. Recent Advancement Made in the Field of Reduced Graphene Oxide-Based Nanocomposites Used in the Energy Storage Devices: A Review. *J Energy Storage* **2021**, *33*, 102032. https://doi.org/https://doi.org/10.1016/j.est.2020.102032.

(10) Yu, W.; Yoshii, T.; Aziz, A.; Tang, R.; Pan, Z.-Z.; Inoue, K.; Kotani, M.; Tanaka, H.; Scholtzová, E.; Tunega, D.; Nishina, Y.; Nishioka, K.; Nakanishi, S.; Zhou, Y.; Terasaki, O.; Nishihara, H. Edge-Site-Free and Topological-Defect-Rich Carbon Cathode for High-Performance Lithium-Oxygen Batteries. *Advanced Science* **2023**, *10* (16), 2300268. https://doi.org/https://doi.org/10.1002/advs.202300268.

(11) Gkika, D. A.; Karmali, V.; Lambropoulou, D. A.; Mitropoulos, A. C.; Kyzas, G. Z. Membranes Coated with Graphene-Based Materials: A Review. *Membranes (Basel)* **2023**, *13* (2). https://doi.org/10.3390/membranes13020127.

(12) Bhol, P.; Yadav, S.; Altaee, A.; Saxena, M.; Misra, P. K.; Samal, A. K. Graphene-Based Membranes for Water and Wastewater Treatment: A Review. *ACS Appl Nano Mater* **2021**, *4* (4), 3274–3293.

(13) Gadipelli, S.; Guo, Z. X. Graphene-Based Materials: Synthesis and Gas Sorption, Storage and Separation. *Prog Mater Sci* **2015**, *69*, 1–60. https://doi.org/https://doi.org/10.1016/j.pmatsci.2014.10.004.

(14) Machado, B. F.; Serp, P. Graphene-Based Materials for Catalysis. *Catal. Sci. Technol.* **2012**, *2* (1), 54–75. https://doi.org/10.1039/C1CY00361E.

(15) Fan, X.; Zhang, G.; Zhang, F. Multiple Roles of Graphene in Heterogeneous Catalysis. *Chem. Soc. Rev.* **2015**, *44* (10), 3023–3035. https://doi.org/10.1039/C5CS00094G.

(16) Prakash, S. H.; Roopan, S. M. A Comprehensive Review on Recent Developments in the Graphene Quantum Dot Framework for Organic Transformations. *J Organomet Chem* **2023**, *997*, 122790. https://doi.org/https://doi.org/10.1016/j.jorganchem.2023.122790.

(17) Gergeroglu, H.; Yildirim, S.; Ebeoglugil, M. F. Nano-Carbons in Biosensor Applications: An Overview of Carbon Nanotubes (CNTs) and Fullerenes (C60). *SN Appl Sci* **2020**, *2* (4), 603. https://doi.org/10.1007/s42452-020-2404-1.

(18) Nag, A.; Mitra, A.; Mukhopadhyay, S. C. Graphene and Its Sensor-Based Applications: A Review. *Sens Actuators A Phys* **2018**, *270*, 177–194.

https://doi.org/https://doi.org/10.1016/j.sna.2017.12.028.

(19) Yusof, N. A.; Abd Rahman, S. F.; Muhammad, A. Chapter 9 - Carbon Nanotubes and Graphene for Sensor Technology. In *Synthesis, Technology and Applications of Carbon Nanomaterials*; Rashid, S. A., Raja Othman, R. N. I., Hussein, M. Z., Eds.; Elsevier, 2019; pp 205–222. https://doi.org/https://doi.org/10.1016/B978-0-12-815757-2.00009-7.

(20) MACKAY, A. L.; TERRONES, H. Diamond from Graphite. *Nature* **1991**, *352* (6338), 762. https://doi.org/10.1038/352762a0.

(21) Iijima, S.; Ichihashi, T.; Ando, Y. Pentagons, Heptagons and Negative Curvature in Graphite Microtubule Growth. *Nature* **1992**, *356* (6372), 776–778. https://doi.org/10.1038/356776a0.

(22) Chi, S.; Kim, C.; Lee, Y.; Choi, M. Diversity in Atomic Structures of Zeolite-Templated Carbons and the Consequences for Macroscopic Properties. *JACS Au* **2024**. https://doi.org/10.1021/jacsau.4c00028.

(23) Taylor, E. E.; Garman, K.; Stadie, N. P. Atomistic Structures of Zeolite-Templated Carbon. *Chemistry of Materials* **2020**, *32* (7), 2742–2752. https://doi.org/10.1021/acs.chemmater.0c00535.

(24) Wang, M.-W.; Fan, W.; Li, X.; Liu, Y.; Li, Z.; Jiang, W.; Wu, J.; Wang, Z. Molecular Carbons: How Far Can We Go? *ACS Nano* **2023**, *17* (21), 20734–20752. https://doi.org/10.1021/acsnano.3c07970.

(25) Zhang, Y.; Yang, D.; Pun, S. H.; Chen, H.; Miao, Q. Merging a Negatively Curved Nanographene and a Carbon Nanoring. *Precision Chemistry* **2023**, *1* (2), 107–111. https://doi.org/10.1021/prechem.3c00009.

(26) Zhang, Y.; Pun, S. H.; Miao, Q. The Scholl Reaction as a Powerful Tool for Synthesis of Curved Polycyclic Aromatics. *Chem Rev* **2022**, *122* (18), 14554–14593. https://doi.org/10.1021/acs.chemrev.2c00186.

(27) Pun, S. H.; Miao, Q. Toward Negatively Curved Carbons. *Acc Chem Res* **2018**, *51* (7), 1630–1642. https://doi.org/10.1021/acs.accounts.8b00140.

(28) Pun, S. H.; Chan, C. K.; Luo, J.; Liu, Z.; Miao, Q. A Dipleiadiene-Embedded Aromatic Saddle Consisting of 86 Carbon Atoms. *Angewandte Chemie International Edition* **2018**, *57* (6), 1581–1586. https://doi.org/https://doi.org/10.1002/anie.201711437.

(29) Cheung, K. Y.; Chan, C. K.; Liu, Z.; Miao, Q. A Twisted Nanographene Consisting of 96 Carbon Atoms. *Angewandte Chemie International Edition* **2017**, *56* (31), 9003–9007. https://doi.org/https://doi.org/10.1002/anie.201703754.

(30) Cheung, K. M.; Xiong, Y.; Pun, S. H.; Zhuo, X.; Gong, Q.; Zeng, X.; Su, S.; Miao, Q. Negatively Curved Molecular Nanocarbons Containing Multiple Heptagons Are Enabled by the Scholl Reactions of Macrocyclic Precursors. *Chem* **2023**, *9* (10), 2855–2868. https://doi.org/https://doi.org/10.1016/j.chempr.2023.05.028.

(31) Chaolumen; Stepek, I. A.; Yamada, K. E.; Ito, H.; Itami, K. Construction of Heptagon-Containing Molecular Nanocarbons. *Angewandte Chemie International Edition* **2021**, *60* (44), 23508–23532. https://doi.org/https://doi.org/10.1002/anie.202100260.

(32) Brakke, K. *Ken Brakke's Home Page*. https://kenbrakke.com/ (accessed 2024-01-18).

(33) Schoen, A. H. *Alan Schoen geometry*. Date accessed: https://schoengeometry.com/e-tpms.html (accessed 2023-12-18).

(34) King, R. B. Chemical Applications of Topology and Group Theory. 29. Low Density Polymeric Carbon Allotropes Based on Negative Curvature Structures. *J Phys Chem* **1996**, *100* (37), 15096–15104. https://doi.org/10.1021/jp9613201.

(35) O'Keeffe, M.; Adams, G. B.; Sankey, O. F. Predicted New Low Energy Forms of Carbon. *Phys. Rev. Lett.* **1992**, *68* (15), 2325–2328. https://doi.org/10.1103/PhysRevLett.68.2325.

(36) Zhu, C.; Shoyama, K.; Niyas, M. A.; Würthner, F. Supramolecular Substructure of C60-Embedded Schwarzite. *J Am Chem Soc* **2022**, *144* (36), 16282–16286. https://doi.org/10.1021/jacs.2c06933.

(37) Kawasumi, K.; Zhang, Q.; Segawa, Y.; Scott, L. T.; Itami, K. A Grossly Warped Nanographene and the Consequences of Multiple Odd-Membered-Ring Defects. *Nat Chem* **2013**, *5* (9), 739–744. https://doi.org/10.1038/nchem.1704.

(38) King, B. T. Nanographenes Do the Twist. *Nat Chem* **2013**, *5* (9), 730–731. https://doi.org/10.1038/nchem.1732.

(39) Kirschbaum, T.; Rominger, F.; Mastalerz, M. A Chiral Polycyclic Aromatic Hydrocarbon Monkey Saddle. *Angewandte Chemie International Edition* **2020**, *59* (1), 270–274. https://doi.org/https://doi.org/10.1002/anie.201912213.

(40) Gao, Q.; Ou, L.; Hu, Z. Architecture Design of Novel Carbon Family: Polyhedra as Building Blocks. *Carbon Trends* **2023**, *11*, 100256. https://doi.org/https://doi.org/10.1016/j.cartre.2023.100256.

(41) Hyde, S. T.; O'Keeffe, M. At Sixes and Sevens, and Eights, and Nines: Schwarzites P3, p = 7, 8, 9. *Struct Chem* **2017**, *28* (1), 113–121. https://doi.org/10.1007/s11224-016-0782-1.

(42) Hyde, S. T.; Cramer Pedersen, M. Schwarzite Nets: A Wealth of 3-Valent Examples Sharing Similar Topologies and Symmetries. *Proceedings of the Royal Society A: Mathematical, Physical and Engineering Sciences* **2021**, *477* (2246), 20200372. https://doi.org/10.1098/rspa.2020.0372.

(43) He, C.; Sun, L.; Zhang, C.; Zhong, J. Two Viable Three-Dimensional Carbon Semiconductors with an Entirely Sp2 Configuration. *Physical Chemistry Chemical Physics* **2013**, *15* (2), 680–684. https://doi.org/10.1039/C2CP43221H.

(44) Wang, Z.; Ke, X.; Zhu, Z.; Zhu, F.; Ruan, M.; Chen, H.; Huang, R.; Zheng, L. A New Carbon Solid Made of the World's Smallest Caged Fullerene C20. *Phys Lett A* **2001**, *280* (5), 351–356. https://doi.org/https://doi.org/10.1016/S0375-9601(00)00847-1.

(45) Ignatchenko, A. V; Willower, J. P. Schwarz P-Surface via Isolated Sp2 Carbon Heptagons: Design and Properties. *J Comput Chem* **2023**, *44* (9), 954–961. https://doi.org/10.1002/jcc.27055.

(46) Blatov, V. A.; O'Keeffe, M.; Proserpio, D. M. Vertex-, Face-, Point-, Schläfli-, and Delaney-Symbols in Nets, Polyhedra and Tilings: Recommended Terminology. *CrystEngComm* **2010**, *12* (1), 44–48. https://doi.org/10.1039/B910671E.

(47) Lenosky, T.; Gonze, X.; Teter, M.; Elser, V. Energetics of Negatively Curved Graphitic Carbon. *Nature* **1992**, *355* (6358), 333–335. https://doi.org/10.1038/355333a0.

(48) Terrones, H.; Terrones, M. Curved Nanostructured Materials. *New J Phys* **2003**, *5*, 126. https://doi.org/10.1088/1367-2630/5/1/126.

(49) Vanderbilt, D.; Tersoff, J. Negative-Curvature Fullerene Analog of C60. *Phys. Rev. Lett.* **1992**, *68* (4), 511–513. https://doi.org/10.1103/PhysRevLett.68.511.

(50) Hoffmann, R.; Kabanov, A. A.; Golov, A. A.; Proserpio, D. M. Homo Citans and Carbon Allotropes: For an Ethics of Citation. *Angewandte Chemie International Edition* **2016**, *55* (37), 10962–10976. https://doi.org/https://doi.org/10.1002/anie.201600655.

(51) Tietze, L. F.; Brasche, G.; Gericke, K. M. Radical Domino Reactions. In *Domino Reactions in Organic Synthesis*; John Wiley & Sons, Ltd, 2006; pp 219–279. https://doi.org/https://doi.org/10.1002/9783527609925.ch3.

(52) Burton, W. K.; Cabrera, N.; Frank, F. C. The Growth of Crystals and the Equilibrium Structure of Their Surfaces. *Philosophical Transactions of the Royal Society of London. Series A, Mathematical and Physical Sciences* **1951**, *243*, 299–358.

(53) Shi, J.; Li, L.; Li, Y. O-Silylaryl Triflates: A Journey of Kobayashi Aryne Precursors. *Chem Rev* **2021**, *121* (7), 3892–4044. https://doi.org/10.1021/acs.chemrev.0c01011.

(54) Chen, L.; Zhang, C.; Wen, C.; Zhang, K.; Liu, W.; Chen, Q. Gold-Catalyzed Cyclotrimerization of Arynes for the Synthesis of Triphenylenes. *Catal Commun* **2015**, *65*, 81–84. https://doi.org/https://doi.org/10.1016/j.catcom.2015.02.029.

(55) Peña, D.; Escudero, S.; Pérez, D.; Guitián, E.; Castedo, L. Efficient Palladium-Catalyzed Cyclotrimerization of Arynes: Synthesis of Triphenylenes. *Angewandte Chemie International Edition* **1998**, *37* (19), 2659–2661. https://doi.org/https://doi.org/10.1002/(SICI)1521-3773(19981016)37:19<2659::AID-ANIE2659>3.0.CO;2-4.

(56) Lutz F. Tietze; Gordon Brasche; Kersten M. Gericke. Pericyclic Domino Reactions. In *Domino Reactions in Organic Synthesis*; John Wiley & Sons, Ltd, 2006; pp 280–336. https://doi.org/https://doi.org/10.1002/9783527609925.ch4.

(57) Rickhaus, M.; Mayor, M.; Juríček, M. Chirality in Curved Polyaromatic Systems. *Chem. Soc. Rev.* **2017**, *46* (6), 1643–1660. https://doi.org/10.1039/C6CS00623J.

(58) *The Credit Goes to Veronica Duell and Megan McMichael*.

(59) Zha, G.-F.; Bare, G. A. L.; Leng, J.; Shang, Z.-P.; Luo, Z.; Qin, H.-L. Gram-Scale Synthesis of β-(Hetero)Arylethenesulfonyl Fluorides via a Pd(OAc)2 Catalyzed Oxidative Heck Process with DDQ or AgNO3 as an Oxidant. *Adv Synth Catal* **2017**, *359* (18), 3237–3242. https://doi.org/https://doi.org/10.1002/adsc.201700688.

(60) Lennox, A. J. J.; Lloyd-Jones, G. C. Selection of Boron Reagents for Suzuki–Miyaura Coupling. *Chem. Soc. Rev.* **2014**, *43* (1), 412–443. https://doi.org/10.1039/C3CS60197H.

TOC

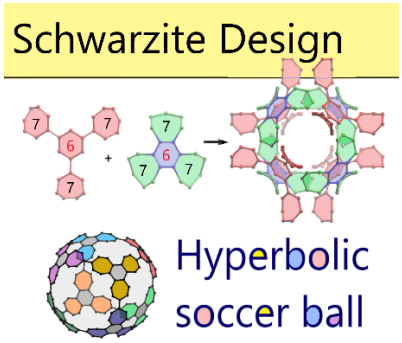

A bottom-up synthesis plan for creating a 3D periodic graphene-like surface from sp^2 carbon heptagon cycles is presented for dozens of Schwarzites. Heptagons are organized in trimers and tiled on gyroid, P, D, CLP, IWP, H, HT, and GW surfaces according to their symmetry. The paradigm shift of the synthetic design lies in creating benzene rings rather than using them as building blocks.